Ultrasonics Sonochemistry 92 (2023) 106283

Contents lists available at ScienceDirect

Ultrasonics Sonochemistry

journal homepage: www.elsevier.com/locate/ultson

Ultrasonic assisted extraction of polyphenols from bayberry by deep eutectic supramolecular polymer and its application in bio-active film

Feng Shi [a], Xiaoping Hai [a], Yun Zhu [a], Lei Ma [a], Lina Wang [a], Jinfang Yin [a], Xiaofen Li [a], Zhi Yang [a], Mingwei Yuan [b], Huabin Xiong [a,*], Yuntao Gao [b,*]

[a] School of Chemistry and Environment, Yunnan Minzu University, Kunming 650504, PR China
[b] National and Local Joint Engineering Research Center for Green Preparation Technology of Biobased Materials, Yunnan Minzu University, Kunming 650504, PR China

ARTICLE INFO

Keywords:
Ultrasonic-assisted extraction
Deep eutectic supramolecular polymer
Polyphenolic of bayberry
Bio-active film
Antioxidant capacity

ABSTRACT

Ultrasound and deep eutectic supramolecular polymers (DESP) is a novel combination of green extraction method for phytochemicals. In this study, a new type of green extractant was developed: DESP. It is a derivative of deep eutectic solvent (DES) and was prepared by supramolecular polymer unit β-cyclodextrin (β-CD) as hydrogen bond acceptor (HBA) and organic acid as hydrogen bond donor (HBD). The current work focuses on the use of ultrasonic-assisted (UAE) DESP extraction of polyphenolic compounds (PCs) from bayberry. The experimental results showed that DESP synthesized with β-CD and lactic acid (LA) in a ratio of 1:1 (w/w %) had the best extraction effect. And by using a three-level factor experiment and the response surface method, the predicted TPC content is very close to the actual content (28.85 ± 1.27 mg GAE/g). The DESP extract including PCs were further used as plasticizer for chitosan (CS) to prepare highly active green biofilms (DESP-CS). It is possible to reduce the tedious procedures for separating biologically active substances from DESP. The experiment proved that the prepared films have good mechanical properties, plastic deformation resistance, thermal stability and antioxidant activity.

1. Introduction

Polyphenolic compounds (PCs) is a diverse and multifunctional plant active substances widely present in plants, containing flavonoids, phenolic acids, anthocyanins, and procyanidins. Because of the properties of antioxidant, antibacterial, antiviral, anti-inflammatory, antidiabetic, and anti-obesity activities [1], polyphenols or polyphenol extracts have been widely used in food, medicine and health care, and other fields. Bayberry is a kind of fruit with a unique flavor, excellent nutrients, and high commercial value [2,3]. However, bayberry is often wasted because it is difficult to preserve, causing serious waste of resources and environmental pollution. In particular, although its extract has great potential application value, the effective functional components of bayberry have not been fully utilized [4]. It has been reported that it has been used in antioxidant, anti-inflammatory, and antidiabetic because of its high content of phytochemicals such as phenolic compounds, anthocyanins, and vitamins [5–7]. Polyphenol composition from bayberry has been determined by the HPLC-DAD-ESI-MS method, and its free radical scavenging ability has been evaluated using different detection methods [8]. Furthermore, a large number of phenolic compounds and high antioxidant activity have been observed [9,10]. At present, several methods, such as traditional organic solvents (formic acid, ethanol), ultrasonic treatment, squeezing, and drying methods, were employed to obtain bayberry extract [11–13]. Unfortunately, these methods are not satisfactory for researchers and consumers owing to the residue of toxic solvents and low efficiency. Therefore, it is extremely urgent to develop a green method of extracting polyphenols with a non-toxic solvent.

Deep eutectic solvents (DES) are considered to be a new class of green solvents with the advantages of non-volatility, chemical stability, non-flammability, and reusability [14], so it has been hailed as the solvent of the 21st century by Paiva [15]. DES is a new generation solvent synthesized by hydrogen bond acceptor (HBA) and hydrogen bond donor (HBD) in different ratios through hydrogen bonding force [16], and its melting point is lower than that of each of its components [17]. Deep eutectic supramolecular polymer (DESP) is a novel derivative of DES and was first reported by Wu in 2021 [18]. DESP combines the covalent interaction mode of supramolecular polymer with the

* Corresponding authors.
E-mail addresses: xionghuabin@ynni.edu.cn (H. Xiong), 040343@ymu.edu.cn (Y. Gao).

https://doi.org/10.1016/j.ultsonch.2022.106283
Received 31 October 2022; Received in revised form 5 December 2022; Accepted 27 December 2022
Available online 28 December 2022

macroscopic state of DES. When the structural unit cyclodextrin (CD) of supramolecular polymer and organic acids were as HBA and HBD respectively, CD-OH and natural acid-COOH can form hydrogen bonds and DESP complexation was prepared at low temperature. In addition, DESP also possesses the properties of DES as a multifunctional medium, which is not only a medium for efficient extraction and stable storage of bioactive components, but also can directly apply to downstream industrial utilization (such as cosmetics and nutritional products, etc.) without separation process like traditional organic solvents [19]. However, the use of DESP as an extractant has not yet been reported and it is believed that DESP will also become a rookie in the field of extractants.

Ultrasonic-assisted extraction (UAE) is based on the principle of acoustic cavitation. The cavitation effect can quickly and efficiently destroy the cell wall of the plant matrix, which helps to release cellular bioactive compounds [20]. Extraction of polyphenolic compounds from bayberry using ultrasound-assisted DESP is a good method for green extraction techniques. As a new derivative of DES, DESP has shown superiority in environmental protection. However, the recovery of biologically active compounds from DESP solution is full of challenges due to the low vapor pressure of DESP [21]. Therefore, to address the difficulty the strategy that DESP extract can be directly applied to enhance the activity of various biofilms is inspired. Chitosan (CS), a natural polysaccharide obtained by deacetylation of chitin, is an important basic material for the preparation of biofilms [22]. The formation of CS film requires an acidic medium as a dissolving agent for CS (such as acetic acid) [23] and the addition of a certain plasticizer (such as glycerol) [24]. DESP can provide an acidic medium for the dissolution of CS and also act as a plasticizer for CS [25]. Therefore, the preparation of degradable biofilm is a good choice for developing further applications of DESP.

The innovation of this research is to take green chemistry as the theme, DESP as a novel extractant was prepared and supplemented by ultrasonic extraction of the active component PCs in bayberry, and blended the DESP extract rich in PCs with CS to prepare high active biofilm (DESP-CS). The primary purpose of this study was to investigate the extraction effects of different kinds of DESPs on PCs and compare with DESP and other extractants. Meanwhile, the extraction rate was optimized with the response surfaces method and the effects of DESP concentration, ultrasound power, and ultrasound time were analyzed using the Box-Behnken design (BBD). The effects of DESP and TPC content on the mechanical properties, thermal properties, and antioxidant activity of DESP-CS were further discussed.

2. Materials and methods

2.1. Chemicals and materials

The bayberry was freeze-dried with a vacuum, pulverized to a particle size of <250 μm and stored in a vacuum bag for future use. Chitosan (<200 mPa.s, CS), β-cyclodextrin (β-CD), Malic acid (MA), Lactic acid (LA), Citric acid (CA), Gallic acid standard, Folin-Ciocalteu reagent, choline chloride (ChCl), 2,2′-azino-bis(3-ethylbenzothiazoline-6-sulfonic acid) (ABTS) standard and 1,1-diphenyl-2-picrylhydrazyl radical (DPPH) standard were purchased from McLean Biochemical Reagent Co., ltd. Shanghai, China. All reagents required for the experiments were of analytical grade.

2.2. Preparation of DESP

To prepare DESP in this study, organic acid was used as HBD, β-CD was selected as HBA. Three organic acids were selected for each DESP as the donors of different hydrogen bonds, and their compositions and ratios are shown in Table 1. The HBA and HBD are mixed in different proportions and then heated to form a stable and uniform transparent liquid as shown in Fig. 1.

Table 1
DESPs prepared from β-cyclodextrin and natural acids in different ratios.

Number	Abbreviation	Composition	Mass ratio
1	DESP-1	β-CD:LA	1:1
2	DESP-2	β-CD:LA	1:2
3	DESP-3	β-CD:LA	1:3
4	DESP-4	β-CD:LA	1:4
5	DESP-5	β-CD:LA	1:5
6	DESP-6	β-CD:CA	1:1
7	DESP-7	β-CD:CA	1:2
8	DESP-8	β-CD:CA	1:3
9	DESP-9	β-CD:CA	1:4
10	DESP-10	β-CD:CA	1:5
11	DESP-11	β-CD:MA	1:1
12	DESP-12	β-CD:MA	1:2
13	DESP-13	β-CD:MA	1:3
14	DESP-14	β-CD:MA	1:4
15	DESP-15	β-CD:MA	1:5

β-CD: β-Cyclodextrin; LA: Lactic Acid; CA: Citric Acid; MC: Malic Acid.

2.3. Ultrasonic-assisted extraction of polyphenols and parameters optimization

Using an ultrasonic processor (DC-2006, Ningbo, China) and a titanium alloy probe (15 mm diameter) to obtain bayberry extract. In detail, bayberry and DESP solution were mixed evenly in a 50 mL beaker and placed in an ice bath, and the pulse sequence interval of the whole extraction process was 2 s ON and 1 s OFF. Some factors such as solid–liquid ratio (1:75–175 g/mL), DESP concentration (10–70 %), the ratio of HBA and HBD (1:1–5 w/w%), ultrasonic power (150–1200 W), and ultrasonic time (5–40 min) were optimized to improve the rate of extraction of bayberry, and then the supernatant was collected by centrifugation (10 min, 4500 rcf) for further analysis, and the optimal TCP extraction factors were screened.

The Box-Behnken design (BBD) was used for in-depth experimental optimization. In this optimization experiment, the independent variables (X) and their levels are: DESP concentration (30–50 %), ultrasonic power (750–1050 W) and extraction time (30–40 min), total phenolic content was used as the dependent variables Y1, Y2 and Y3 of BBD experiment to evaluate the response. And the influence of the independent variable (X) was analyzed by RSM. The codes are shown in Table S1. The predicted response was calculated by the second-order polynomial model shown in Eq. (1) [26]:

$$Y = \beta_0 + \sum_{i=1}^{3} \beta_i X_i + \sum_{i=1}^{3} \beta_{ii} X_i^2 + \sum_{i=0}^{3} \sum_{j=i+1}^{3} \beta_{ij} X_i X_j \quad (1)$$

where Y is the response; X_i and X_j are independent variables; and β_0, β_i, β_{ii}, and β_{ij} are the regression coefficients for the intercept, linear, quadratic, and interaction effects, respectively.

2.4. Preparation of DESP-CS

DESP-CS were prepared with the above-obtained bayberry extract according to the method reported by Roy with slight modifications [27]. Specifically, the bayberry extract was mixed with CS in a 50 mL beaker and stirred until CS was completely dissolved to obtain a homogeneous mixture of DESP-CS, and then placed in a polytetrafluoroethylene mold to dry naturally under vacuum conditions to obtain DESP-CS. A blank control of bioactive film (DESP-CS-K) was prepared with original DESP instead of bayberry extract. Its composition and proportion are shown in Table 2.

2.5. Determination of total polyphenol content in the extract

The determination of TPC in bayberry extract was based on the Folin-Ciocalteu colorimetric method used by Wu with a slight modification

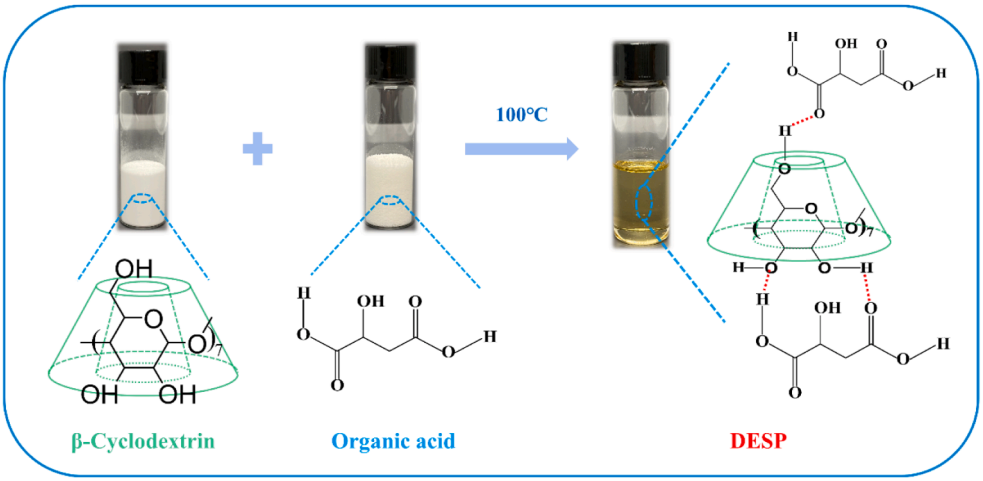

Fig. 1. Preparation process of DESP.

Table 2
Biofilms prepared from DESP and chitosan in different ratios.

Biofilms	Abbreviation	Chitosan (g)	DESP (mL)	H_2O (mL)
Sample films	DESP-CS-1	0.3000	1.00	19.00
	DESP-CS-2	0.3000	2.00	18.00
	DESP-CS-3	0.3000	3.00	17.00
	DESP-CS-4	0.3000	4.00	16.00
	DESP-CS-5	0.3000	5.00	15.00
	DESP-CS-6	0.3000	20.00	0.00
Control films	DESP-CS-K1	0.3000	1.00	19.00
	DESP-CS-K2	0.3000	2.00	18.00
	DESP-CS-K3	0.3000	3.00	17.00
	DESP-CS-K4	0.3000	4.00	16.00
	DESP-CS-K5	0.3000	5.00	15.00
	DESP-CS-K6	0.3000	20.00	0.00

[28]. Briefly, 100 μL of the extract was mixed with 6.4 mL distilled water, 0.5 mL FC reagent, and 3 mL of Na_2CO_3 solution (10 % w/v) by vortexing, and the absorbance was recorded at λ = 765 nm after incubation at 35 °C for 60 min. A calibration curve was drawn for gallic acid. TPC is represntatived with milligrams of gallic acid equivalents (GAE) per gram of sample dry weight (mg GAE/g).

2.6. Characterizations

DESP nuclear magnetic resonance (^{1}H NMR) was detected using FT NMR 400 MHz (BRUKER AV III-400, USA) to find the changes in hydrogen bonding during the synthesis. The Changes of functional groups in DESP and DESP-CS were detected by FT-IR (NICOLET iS10, USA.) at 500–4000 cm^{-1}. The thermal stability of DESP and DESP-CS were analyzed using TGA (STA449F3, Germany) at a heating rate of 10 °C/min from 25 to 790 °C in a nitrogen atmosphere. SEM images of DESP, DESP-CS, and bayberry samples were acquired using a field emission scanning electron microscope (FEI Quanta200, USA) under a high vacuum at an accelerating voltage of 10 kV and a working distance of 12.5 mm. The lattice of the samples was analyzed using an X-ray diffractometer (XRD) in the range of 4-70° (35 kV, 30 mA).

2.7. Properties of biofilms

2.7.1. Mechanical properties and transparency of biofilms

The biofilms were cut into strips of a certain length and width, and the thickness of the DESP-CS was measured using a micrometer screw (4202000–25, China). And Young's modulus (MPa), tensile strength (MPa), and elongation at break (%) of the films were measured using an electronic universal testing machine (CMT4104, China). The opacity of the films was determined using a UV–vis spectrophotometer. Films were cut to the appropriate size and fixed on the grooves, then scanned at the wavelength of 200–800 nm. The opacity of the bioactive film is calculated according to Eq. (2):

$$The\ opacity\ =\ \frac{\lambda_{600}}{x} \tag{2}$$

where λ_{600} is the absorbance of the film at 600 nm and x is the thickness of the film.

2.7.2. Analysis of antioxidant activity

The 50 μL of combination of chitosan and bayberry extract was added to 5 mL of ABTS + radical and 5 mL of DPPH• radical methanol solution, respectively. The reaction was protected from light for 30 min, and the absorbance was measured at λ = 734 nm and λ = 517 nm, respectively. The antioxidant capacity of the sample (DPPH and ABTS scavenging activities of bayberry extract) can be calculated using Eq. (3):

$$Antioxidant\ activity(\%)\ =\ \frac{A_0 - A_1}{A_0} \times 100 \tag{3}$$

where A_0 is the absorbance value of the control solution, A_1 is the absorbance value of the sample.

2.7.3. Adhesion strength of biofilms

The bioactive film was cut into suitable long strips, sprayed water fog on both sides of the film evenly, then attached rectangular aluminum alloy sheets, PTFE sheets, and glass sheets, and evaluated quantitatively the adhesion strength of DESP-CS with lap shear adhesion test. The adhesion strength of the film was measured using an electronic universal tester.

2.8. Statistical analysis

RSM optimization was performed using Design-Expert software (version 8.0.6), all graphs were drawn using Origin (version 2018, USA), ^{1}H NMR data analysis was performed using Delta NMR Processing and Control software (V5.3.1), and analysis of one-way ANOVA was used SPSS software (version 18.00).

3. Results and discussion

3.1. Univariate analysis of influencing TPC extraction rate

Fig. 2 shows the effects of different solid–liquid ratios, DESP concentration, the mass ratio of HBA/HBD, ultrasonic power, and extraction time on the TPC of bayberry extract. Under the condition of DESP concentration of 10 %, HBA: HBD of 1:4 (w/w%), ultrasonic power of 600 W, and extraction time of 5 min, screening experiments with five different solid–liquid ratios were carried out. The results showed when solid–liquid ratio was 1:75 (g/mL), the TPC content in the extract (11.28 mg GAE/g) was higher than that of other solid–liquid ratios. It is inferred if the number of extractants increases, the sample can be dispersed enough in the extractant, but the ultrasonic power will be absorbed and decreased for the overburden solvent volume [29]. DESP concentrations were an important factor affecting the extraction of TPC. An appropriate amount of water can reduce the viscosity of DESP and improve the mass transfer performance, thereby increasing the extraction efficiency of natural active ingredients [30]. Under the condition of the HBA: HBD of 1:4 (w/w%), the ultrasonic power of 600 W, the extraction time of 5 min, and the DESP concentration of 40 %, TPC can reach the highest value (17.24 mg GAE/g). The ratio of DESP will affect its performance, such as viscosity, density, polarity, and hydrogen bond content [31].

Moreover, based on the β-CD: LA ratio of 1:1 TPC extraction rate can reach 18.88 mg GAE/g because of lower viscosity and a lot of number of hydrogen bonds. The choice of ultrasonic power and time were important parameters to control the cavitation and mass transfer effects, which can destroy the cell wall of bayberry and make TP diffuse into the DESP [32]. However, with the increase of power and time, the extraction of TP will be negatively affected, which is the reason that TPC is easily suffered from the high temperature of cavitation to decompose [33].

3.2. Kinetic model of ultrasound-assisted DESP extraction

The second-order rate law is most appropriate to elaborate the kinetic model of the fitted ultrasound-assisted extraction process [34]. Using the second-order rate law, the dissolution rate of TPC contained in bayberry from plant cells to solution can be described by Eq. (4):

$$\frac{dC_t}{dt} = k(C_s - C_t)^2 \tag{4}$$

where k is the second-order extraction rate constant (mg/g min), C_t is the concentration of total polyphenols in the liquid extract at a given extraction (mg GAE/g) time t (min), and C_s is the concentration of TPC at equilibrium in liquid extraction (mg GAE/g).

Eq. (5) is obtained by integrating t (t = 0 to t) and C_t (C_t = 0 to C_t) under initial conditions to boundary conditions, so as to determine the parameters of the dynamics.

$$C_t = \frac{C_s^2 kt}{1 + C_s kt} \tag{5}$$

linearized in the form of Eq. (5) to obtain Eq. (6):

$$\frac{t}{C_t} = \frac{1}{kC_s^2} + \frac{t}{C_s} = \frac{1}{h} + \frac{1}{C_s}t \tag{6}$$

where h is the initial extraction rate (mg/g min) when t and C_t are close to 0, and the concentration of TPC at any time can be obtained by rearranging Eq. (6), expressed by Eq. (7):

$$C_t = \frac{t}{(1/h) + (t/C_s)} \tag{7}$$

where h, k and C_s are experimentally determined by plotting t/C_t and t using slope and intercept.

The secondary extraction kinetics of TPC from different kinds of

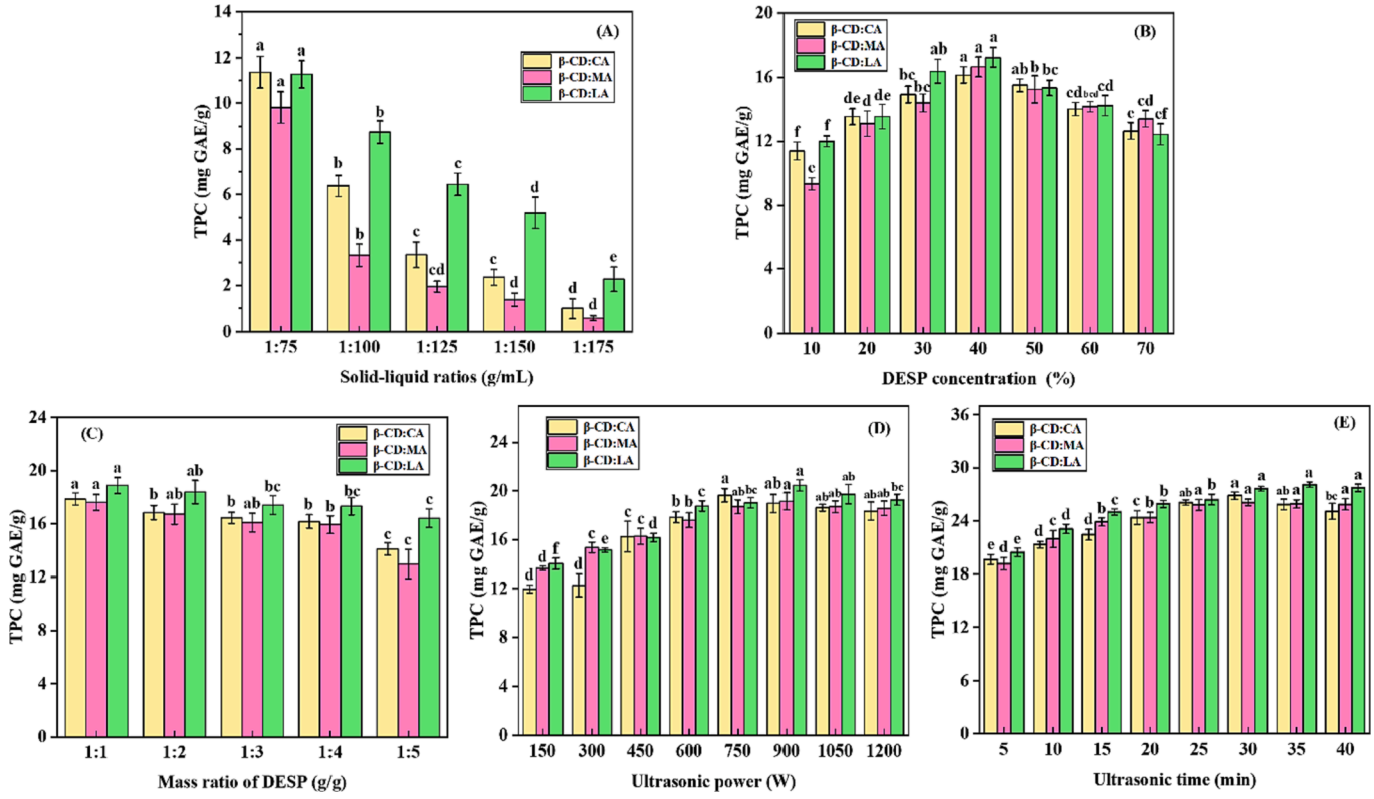

Fig. 2. Effects of each factor on the extraction of TPC: (A) solid–liquid ratio of DESP; (B) DESP concentration; (C) mass ratio of DESP; (D) ultrasound power; (E) ultrasound time.

DESPs were studied, as presented in Fig. 3.

In Fig. 3 (A), the extraction rate of the TPCs was initially very fast, but slowed down over the next extraction time, stabilising and reaching a plateau at 35 min. When the sample was in pure solvent, ultrasound destroyed the surface structure of the bayberry cells, the intracellular TPC rapidly bonded to the hydrogen bonds in the DESP and dissolved in the extractant, which allowed them to be extracted rapidly and also indicated a high initial extraction rate. Furthermore, within 5–10 min ultrasound can provided a strong mass transfer effect to the extraction system [34], which was a major factor in the diffusion of polyphenolic compounds into the solvent. However, when the polyphenolic compounds in bayberries dissolved in the extractant achieve the maximum amount, their polyphenol yields remained at the same level even the time was extended.

The experimental data for the secondary kinetic model of ultrasonic extraction of polyphenolic compounds are plotted in the specific coordinates shown in Fig. 3 (B) and the equations of the fitted curves are shown in Table 3. The specific kinetic parameters are listed in Table 4, including extraction capacity (equilibrium concentration - C_s), extraction rate constant (k) and initial extraction rate (h) determined from Eq. (6) and the linear regression equation for each medium. The secondary kinetic model regression coefficient R^2 was>0.99 ($R^2 > 0.99$) for all experimental data for all extraction media, which implies that the experimental data and the secondary kinetic model predictions are consistent, indicating that the secondary kinetic model is applicable to this study.

3.3. Optimization of extraction parameter

Table 5 shows the ANOVA results for the quadratic polynomial model considering the extracted variables. The effects of different extraction factors were analyzed for each response factor. The significance of every coefficient is determined by the *F*-value and *p*-value. The *F* obtained from the model was 5.0, while the *p* was 0.0227, and higher *F* and lower *p* were associated with more significant correspondence between multiple independent variables [35]. Insignificant terms ($P > 0.05$) were removed to analyze the effect of each independent variable on the TP extracted from the bayberry, resulting in a second-order polynomial Eq. (8):

$$Y_1(\text{TPC, mg GAE/g}) = 28.94 + 0.33A\text{-}0.33B^2\text{-}0.36C \quad (8)$$

The regression coefficient (R^2) of the quadratic polynomial equation for the relationship between the respective variables and the extract of TP was 0.8653, and the R^2 value was considered suitable for such models [36–38].

Response surfaces and 3D plots (Fig. 4) show the effects of DESP concentration, ultrasonic power, and time on the amount of TPC

Table 3
Second-order extraction kinetic equations for ultrasound-assisted extraction of TPC from different DESPs.

Types of DESP	$t/C_t = 1/h + t/C_s$	R^2
β-CD:LA	$t/C_t = 0.0916 + 0.0335\ t$	0.998
β-CD:MA	$t/C_t = 0.0836 + 0.0362\ t$	0.999
β-CD:CA	$t/C_t = 0.0858 + 0.0364\ t$	0.992

Table 4
Parameters of the second-order kinetic model for the extractions of TPC with different DESPs.

Types of DESP	k(mg $g^{-1}min^{-1}$)	h(mg $g^{-1}min^{-1}$)	C_s(mg GAE/g)
β-CD:LA	0.0138	10.9206	28.1373
β-CD:MC	0.0156	11.9560	27.6472
β-CD:AC	0.0154	11.6564	27.4801

Table 5
Analysis of variance (ANOVA) and fitting parameters of the quadratic polynomial model for selected parameters of bayberry extraction.

Source	Total polyphenol contents ($R^2 = 0.8653$)				
	SS	DF	MS	*F*-value	*p*-value
Model	2.400	9	0.2700	5.000	0.0227
A	0.870	1	0.8700	16.320	0.0049
B	0.100	1	0.1000	1.940	0.2064
C	0.014	1	0.0140	0.260	0.6291
AB	0.040	1	0.0400	0.750	0.4154
AC	0.020	1	0.0200	0.370	0.5637
BC	6.250E-004	1	6.250E-004	0.012	0.9169
A^2	0.190	1	0.1900	3.540	0.1021
B^2	0.470	1	0.4700	8.810	0.0208
C^2	0.560	1	0.5600	10.470	0.0144
Lack of fit	0.026	3	0.0088	0.100	0.9552
Pure error	0.350	4	0.8700		

SS, sum of squares. DF, degree of freedom. MS, mean square. Significance level $p =< 0.05$.

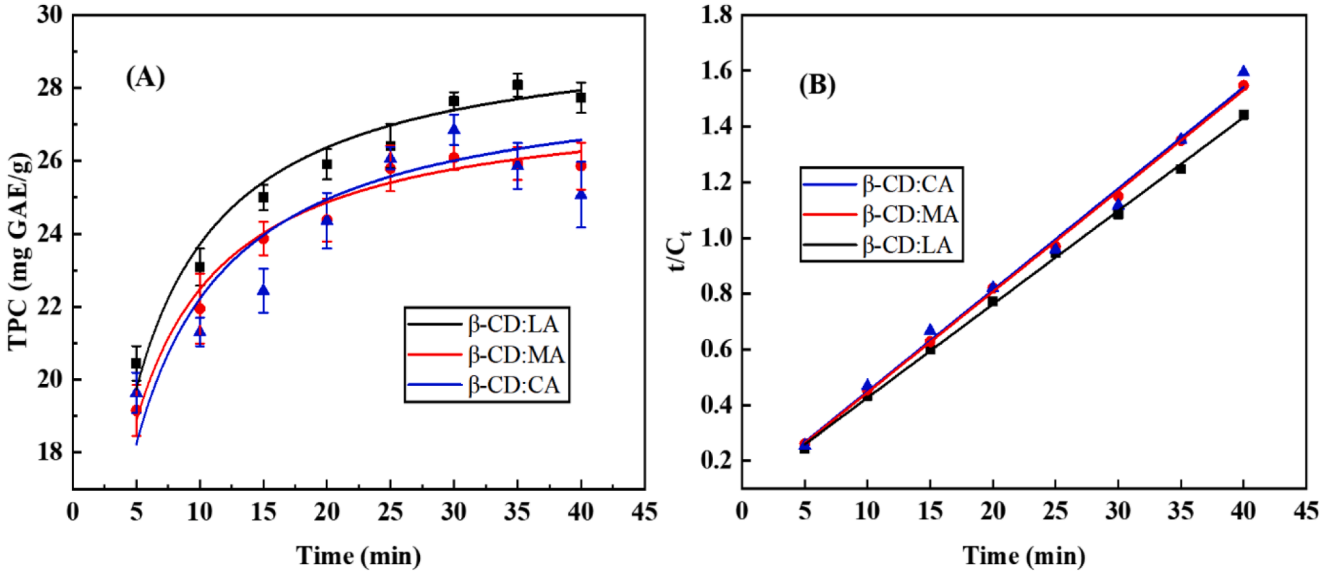

Fig. 3. (A) Influence of DESP species on TPC extracted from bayberry in ultrasounds assistance; (B) Validation of the second-order kinetic model.

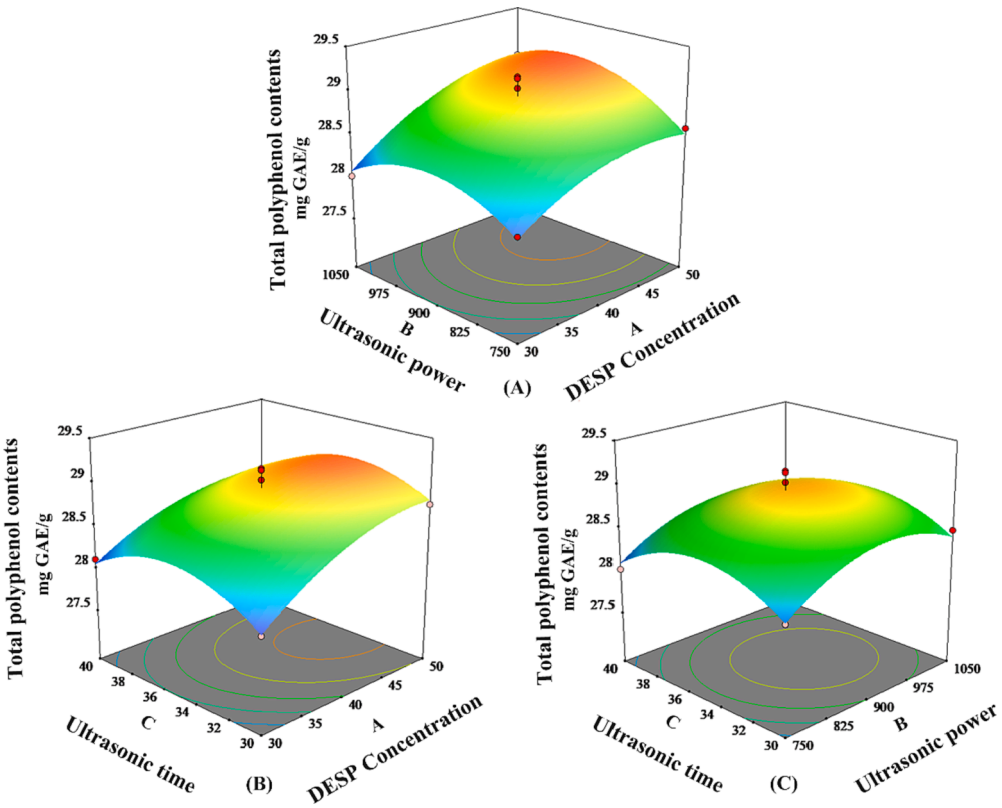

Fig. 4. Total polyphenolic content (TPC, mg GAE/g) of bayberry extracts as a dependent variable of the combination of the independent variables: (A) ultrasonic power and DESP concentration, (B) ultrasonic time and DESP concentration, and (C) ultrasonic time and ultrasonic power.

extracted. Several variables were used to optimize the desirability function [39]. In this experiment, Derringer's desirability function was used to optimize the extraction rate of TP of bayberry. The model predicted the following extraction parameters: DESP concentration of 50 %, ultrasonic power of 948.34 W, and ultrasonic time of 34.21 min. The predicted extraction amount of bayberry TP was 29.097 mg GAE/g. The optimal conditions predicted by the model have carried out the actual experiment. To facilitate the acquisition of experimental conditions, the actual experiment selected DESP concentration of 50 %; ultrasonic power of 948.00 W, extraction time of 35.00 min, and the actual extraction amount of TP was 28.85 ± 1.27 mg GAE/g, which is close to the predicted extraction amount of bayberry TP by the model. Therefore, the ultrasound-assisted DESP is an excellent alternative method to traditional TP extraction methods.

Meanwhile, Fig. S1 shows the extraction effect of DESP with different extractants on polyphenols, and DESP showed a superior extraction

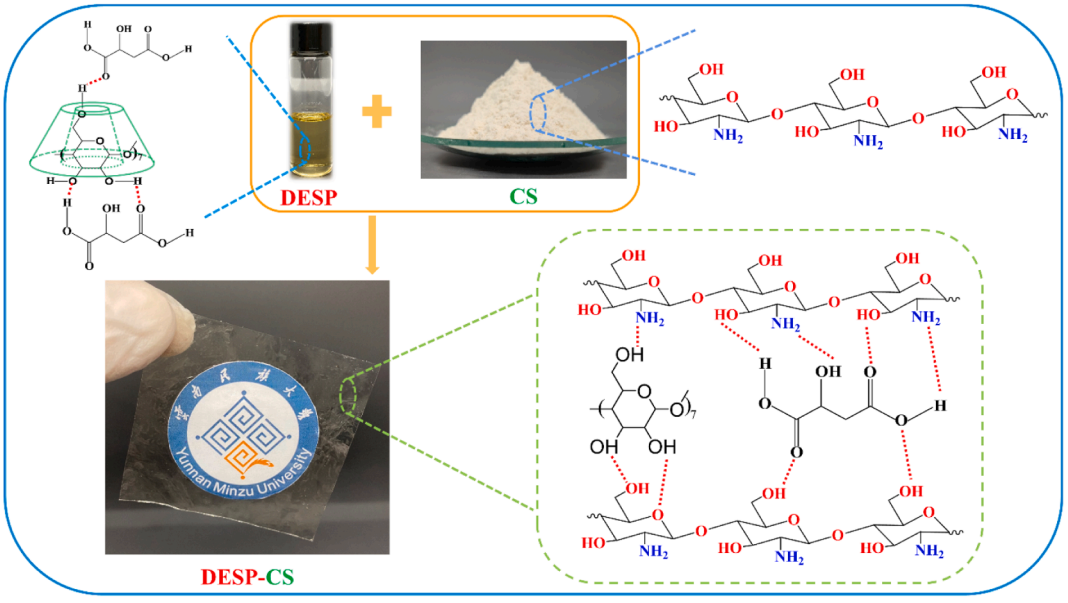

Fig. 5. Mechanism of DESP-CS formation.

effect.

3.4. Preparation of bioactive film

DESP can be used as a green plasticizer for the preparation of film-forming solutions for chitosan. The prepared films with bayberry extracts can not only increase physicochemical, mechanical properties, and biological activities for packaging materials. The separation and recovery of biologically active compounds from DESP extracts is one of the challenging problems. However, it is a new idea that the recovery of bioactive compounds should not be a necessary step, and the complexation may further apply in some fields such as packing and medical materials.

During the extraction process, DESP forms hydrogen bonds with bioactive substances and becomes a storage medium improving the stabilization of bioactive [40]. At the same time, Fig. 5 revealed the mechanism of preparation of DESP-CS. The β-CD and organic acids in the extract (DESP) can form hydrogen bonds with the –NH_2 and –OH groups in CS, allowing the CS film to be completely dissolved in the extract [41]. In Fig. S2 the developed DESP-CS exhibited characteristics of uniform flatness, smoothness, and translucency.

3.5. Antioxidant activity analysis

The content of bioactive components and the antioxidant capabilities are the important basis for the application of biofilms in practice. Therefore, the degradation of polyphenols should be avoided as much as possible during the storage process. The main measures that can be taken are vacuum packaging, avoiding sunlight, and placing in a cool environment and etc. In this paper, the biological activity of DESP-CS was also evaluated by measuring TPC and antiradical capabilities, and the results are shown in Table 6.

The TPC in the sample film was affected by the amount of DESP added. With the increase of the amount of DESP, the amount of TP in the film also increased. Moreover, it was observed that with the increase of DESP extract, the antiradical capabilities of the film were also enhanced. The amount of TPC in the sample film (DESP-CS-1) adding 1 mL of DESP was 1.67 mg GAE/g, and the ABTS + and DPPH· scavenging activities were 62.57 % and 29.51 %, respectively. Accordingly, when 20 mL of DESP extract was added, the three indexes increased to 3.51 mg GAE/g, 87.36 %, and 60.3 %, respectively, which enough demonstrated the ability of DESP-CS to store different contents of natural active ingredients. Different kinds and concentrations of natural active ingredients can be directly added during the preparation of the film, which makes the DESP-CS has great potential for application in any desired field. For example, the incorporation of bioactive ingredients into biopolymer films can enhance the functionality of packaging materials and extend the shelf life of foods [27].

3.6. Characterizations analysis

3.6.1. FTIR and NMR analysis

Fig. 6 shows the FT-IR spectra of DESP, CS, DESP-CS-1, and DESP-CS-K1 (control). The FT-IR spectra of DESP-CS-1 and DESP-CS-K1 showed almost identical patterns. Stretching vibrations of the O—H and N—H groups of DESP and CS were observed in the range of 3391.66 to 3438.02 cm^{-1}, but only one combined bond was shown due to the overlap in the O—H and N—H bonds of the DESP and CS molecules [42]. Moreover, DESP-CS-1 and DESP-CS-K1 have almost the same properties as DESP and CS. Two weak peaks from 2875 to 2987 cm^{-1} were observed in all substances, both manifested as C—H bond stretching vibrations. In CS, the C═O bond has obvious stretching vibration at 1623 cm^{-1}, which is due to the influence of –OH in DESP during film formation, which makes the C═O of CS red-shift [27]. DESP showed C—O—H and C—O—C vibrations at 1039 cm^{-1}, while C—O—H and C—O—C vibrations at 1032 to 1041 cm^{-1} in DESP-CS occurred a slight blue shift, which may be due to the difference between CS and DESP hydrogen bonding between them. The FT-IR spectra of DESP-CS were a composite of DESP and CS spectra. Owing to the acidic characteristics of DESP and the existence of hydrogen bonds, the characteristic peaks of the biofilms are shifted.

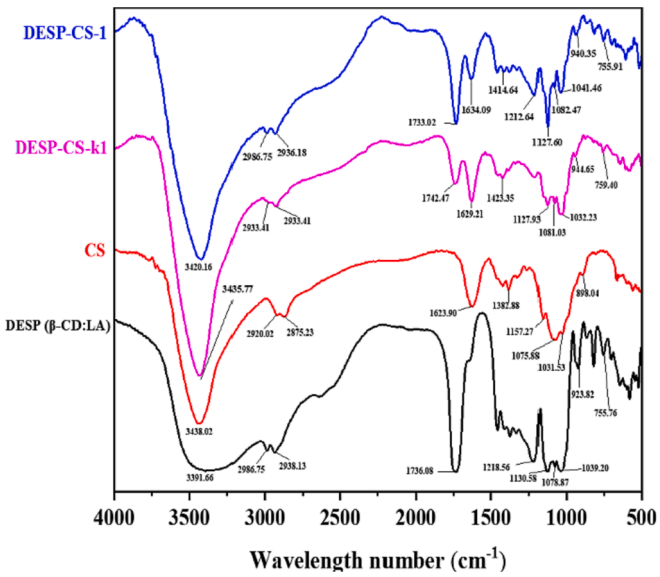

Fig. 6. FTIR of DESP extracts, CS, and DESP-CS.

The comparative ^1H NMR spectra of DESP and constituent components (β-CD and organic acids) are shown in Figs. S3–S5. The obtained spectra confirmed that the formation of DESP is a physical process and no new chemical bonds are formed during its synthesis, which is consistent with the findings of Wu [18].

3.6.2. TG analysis

A thermogravimetric analyzer (TG) was used to analyze the thermal stability of DESP. It is seen from Fig. 7 (A) (Fig. S6) that weight loss of DESP (β-CD/LA) can be divided into three stages. The first stage is between 50 and 150 °C and in this stage bound water of the sample may be removed. The second stage is from 150 °C to 250 °C and the lactic acid in the sample begins to decompose. Between 250 and 700 °C is the third stage and decomposition of β-CD in DESP occurred in this stage. The weight loss of the DESP-CS was the same as the number of the stage with DESP (Fig. 7 (B)). There are also three main stages (Fig. S7). When the temperature was increased from 50 °C to 100 °C, bound water was removed from CS in biofilms [25]. In the next stage (100–200 °C) plasticizer (DESP) in the biofilm bioactive film could start to break down. The decomposition of chitosan acetylation and deacetylation unit components occurred in the third stage (200–700 °C) [18]. Until now, it can speculate that better thermal stability of the biofilms is origin from the presence of plant active components (such as polyphenolic compounds) in the films.

Table 6
The TPC content and ABTS + and DPPH· scavenging activities in various DESP-CS.

Bioactive film	TPC (mg GAE/g)	Antiradical ABTS+ capabilities (%)	Antiradical DPPH· capabilities (%)
DESP-CS-1	1.67 ± 0.16d	62.57 ± 2.14e	29.51 ± 2.67e
DESP-CS-2	2.40 ± 0.14c	67.40 ± 1.68d	41.3 ± 1.54d
DESP-CS-3	2.74 ± 0.23bc	75.21 ± 2.09c	48.4 ± 1.83c
DESP-CS-4	2.94 ± 0.17b	80.44 ± 1.43b	54.3 ± 2.26b
DESP-CS-5	3.07 ± 0.34b	82.12 ± 1.11b	56.1 ± 1.89ab
DESP-CS-6	3.51 ± 0.15a	87.36 ± 2.76a	60.3 ± 2.44a

±, indicates the standard deviation from the mean (n = 3).

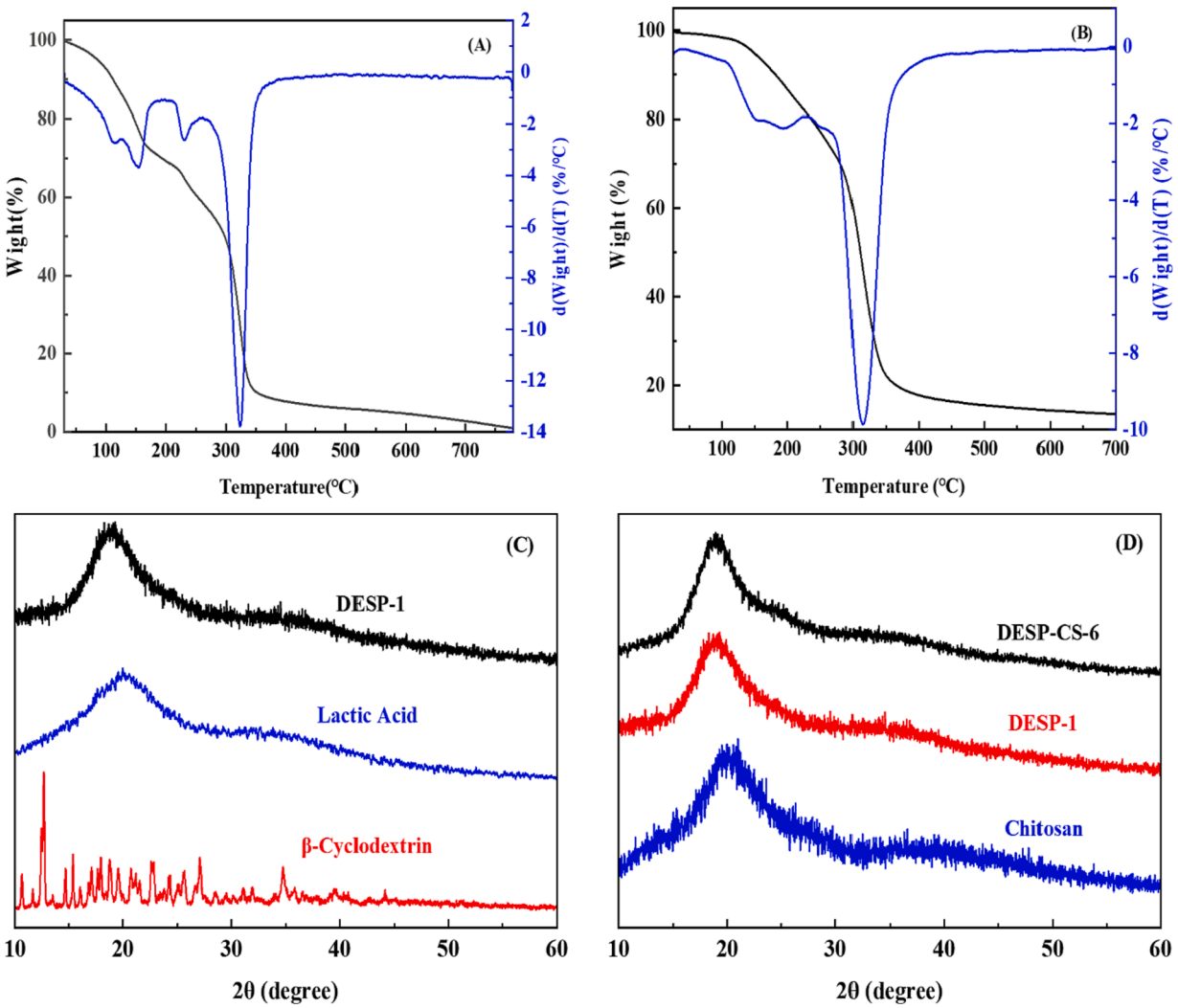

Fig. 7. TG analysis of (A) DESP-1, (B) DESP-CS-6, and XRD analysis of (C) DESP-1, (D) DESP-CS-6.

3.6.3. XRD analysis

In the XRD patterns of different DESP (Fig. 7 (C) and Fig. S8) and DESP-CS (Fig. 7(D) and Fig. S9). Fig. 7 (C) demonstrates the change in crystal shape during the formation of DESP-1. The characteristic peaks are assigned at 12°, 14°, 15°, 17°, 19°, 21°, 22°, 24°, 27° for β-CD respectively [43]. Hydrogen bonds are formed within the lactic acid due to unique liquid properties, resulting in a broader diffraction peak at 20°. During the formation of DESP, β-CD forms a hydrogen bonding system with lactic acid, causing the sharp and intense peaks in β-CD to disappear and tend to be amorphous. The broad peak of chitosan at 20° is a known diffraction peak, which is characteristic of chitosan caused by hydrogen bonding between amino and hydroxyl groups [44]. During the formation of DESP-CS, hydrogen bonds are formed between DESP and CS, while the acidity of DESP makes CS completely soluble in the DESP extract, causing DESP-CS to exhibit an amorphous structure [45].

3.6.4. SEM analysis

The microstructure of the DESP and biofilm before and after preparation were analyzed by SEM. As shown in Fig. 8 (A-C), the DESP based β-CD formed a dense, non-porous, and uniformly transparent morphology, which confirmed the successful synthesis of DESP. It can be seen from Fig. 8 (D),8 (E) and Fig. S10 that the surface microstructure of the DESP-CS was smooth, uniform, dense, and void-free. It is important that the DESP extract, as a green plasticizer, not only provided the necessary acidic medium for dissolving CS [46], but also did make CS completely dissolved in DESP at room temperature, and prepared DESP-CS exhibited to smooth and flat. Moreover, the hydrogen bonds in DESP and DESP extract can be bonded with CS molecules, resulting in a uniform and dense active film without voids.

3.7. Performance analysis of biofilms

3.7.1. Mechanical properties and opacity of biofilms

The mechanical resistance and flexibility of films are usually expressed in terms of Young's modulus (YM), tensile strength (TS), and elongation at break (EB), respectively. According to Table 7, the different DESP contents in the longitudinal direction that the sample film and the control film exhibited the same mechanical properties. With the increase of DESP content, the YM and TS values of the sample film and the control film were decreased, but the EB value was increased. This indicates that DESP can act as a plasticizer to break the original spatial structure of CS, and increases the number of hydrogen bonds, thereby reducing the rigidity of the biofilm and enhancing the plastic deformation resistance of the polymer chain [47].

With the view of the same DESP content, it can be founded that the YM of DESP-CS-1 and DESP-CS-k1 are 1592.68 MPa and 1687.55 MPa, TS is 11.52 MPa and 12.48 MPa, and EB is 1.15 % and 0.92 %, respectively. These results showed that the YM and TS of the sample film were decreased compared with the control film, but the EB value was the opposite. The mechanical properties of the sample film and the control

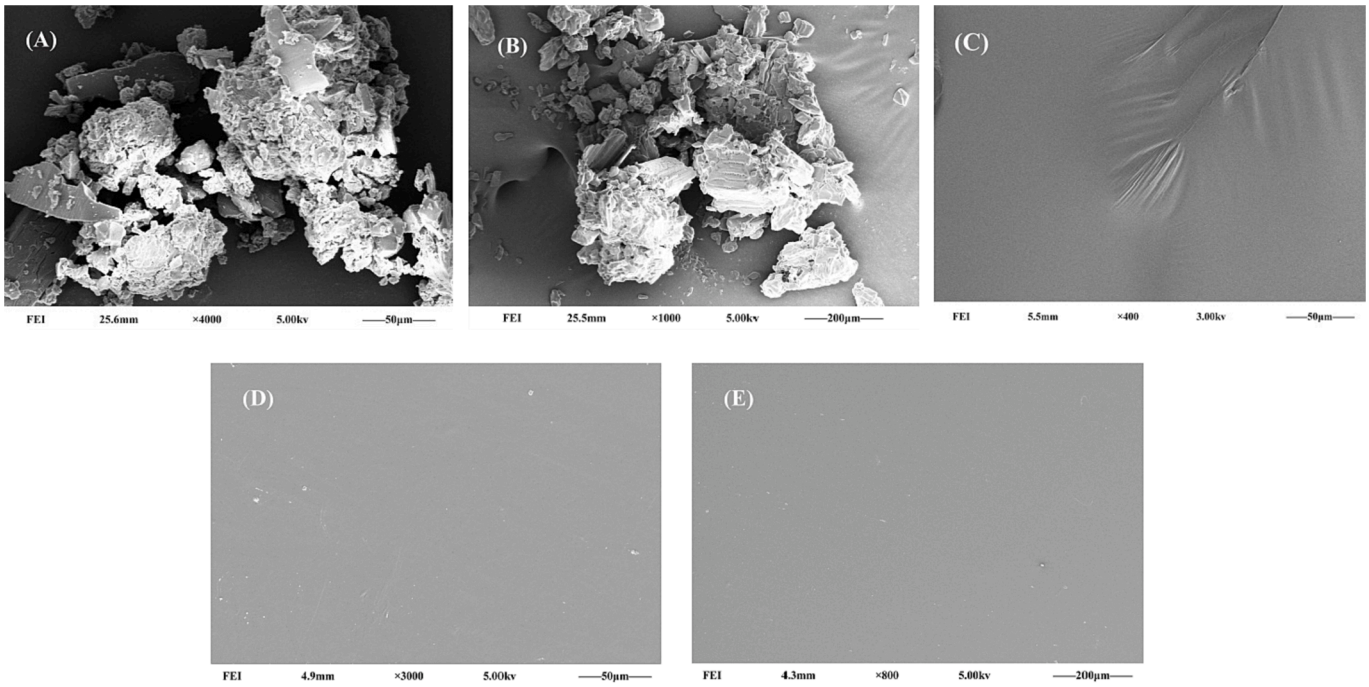

Fig. 8. SEM images of DESPs and DESP-CS: (A) β-cyclodextrin, (B) malic acid, (C) DESP-15, (D) DESP-CS-6, (E) DESP-CS-K6.

Table 7
Mechanical properties and opacity of various DESP-CS.

Biofilms Species		Thickness /mm	Young's modulus (YM)/MPa	Tensile strength (TS)/MPa	Elongation at break (EB)/%	Opacity λ600/x
Sample films	DESP-CS-1	0.074 ± 0.68ab	1592.68 ± 1.17b	11.52 ± 0.84ab	1.15 ± 0.68e	0.84 ± 0.14ef
	DESP-CS-2	0.062 ± 0.79bc	1438.14 ± 2.83d	10.94 ± 1.16adc	4.24 ± 0.94cde	0.89 ± 0.29de
	DESP-CS-3	0.077 ± 0.83a	512.41 ± 1.96 g	7.98 ± 0.69cde	6.17 ± 1.73 cd	1.05 ± 0.35 cd
	DESP-CS-4	0.063 ± 0.56abc	480.26 ± 0.74 h	6.09 ± 1.25de	7.19 ± 1.84c	1.22 ± 0.67bc
	DESP-CS-5	0.056 ± 0.88c	153.94 ± 2.69j	2.77 ± 1.33 fg	8.57 ± 2.11c	1.32 ± 0.24b
	DESP-CS-6	0.061 ± 1.03bc	12.26 ± 1.30 l	0.15 ± 2.06 g	357.9 ± 3.89a	3.72 ± 0.33a
Control films	DESP-CS-K1	0.073 ± 0.77ab	1687.55 ± 2.27a	12.48 ± 1.55a	0.92 ± 1.44e	0.48 ± 0.27f
	DESP-CS-K2	0.072 ± 1.11ab	1573.69 ± 1.86c	12.32 ± 1.74a	2.06 ± 2.35de	0.65 ± 0.39f
	DESP-CS-K3	0.068 ± 1.04abc	669.62 ± 2.33e	8.87 ± 2.39bcd	4.35 ± 0.78cde	0.61 ± 0.42f
	DESP-CS-K4	0.064 ± 0.56abc	573.68 ± 1.52f	7.44 ± 1.27de	6.77 ± 2.12c	0.59 ± 0.81f
	DESP-CS-K5	0.071 ± 0.83abc	386.55 ± 2.64i	5.37 ± 2.06ef	7.44 ± 2.47c	0.58 ± 0.77f
	DESP-CS-K6	0.069 ± 0.77abc	83.45 ± 1.58 k	2.66 ± 2.77 fg	283.56 ± 3.55b	0.68 ± 0.69f

±, indicates the standard deviation from the mean (n = 3).

film were close to the TP in the extract, indicating that the added TP could further improve the rigidity and enhance the plastic deformation resistance of the bioactive film, which is consistent with the conclusion of Xue [48].

By measuring the opacity of the film, the results showed a low λ600/x value, elaborating that the bioactive film has high light transmittance, uniform and transparent characteristics, which is consistent with the results shown in Fig. 4. In summary, the developed DESP-CS is a selective bioactive film that can be prepared by controlling the addition amount of DESP and the content of bioactive substances and has the broad potentials be used in the fields of food preservation, drug packaging, and biomedicine.

3.7.2. Adhesion strength of the DESP-CS

DESP-CS with moisture showed a certain adhesive strength and can be developed as a new type of green bio-glue. The adhesion effect of DESP-CS can be attributed to the cohesive effect (hydrophilic polymerization process of supramolecules, intrinsic factor) and adhesion effect (interaction with surface, extrinsic factor) of DESP [18]. The adhesion strength of DESP-CS on different non-animal tissue substrates is shown in Fig. 9 (A), all DESP-CS exhibited high adhesion strength on hydrophilic surfaces, including glass (3.24 MPa) and iron (2.32 MPa). In contrast, the hydrophobic polytetrafluoroethylene showed lower adhesion strength (0.35 MPa), which is also the main reason for using PTFE as the mold in the film forming process. It is worth noting that the adhesion strength of DESP-CS is consistent with the conclusion obtained in 3.7.1, both the addition of DESP and TPC can improve the adhesion strength of DESP-CS.

To adhere the various tissues together, it is excited that the DESP-CS was placed on the surface of two different tissues, then make the two tissues together. After pressing for about 20 s, the two pieces of separated tissue are glued together. As shown in Fig. S11, the use of DESP-CS can quickly and firmly adhere tissues such as pork, pork skin, and pork chops together. Meanwhile, the adhesion strength of DESP-CS on different animal tissue substrates is shown in Fig. 9 (B), and the results are consistent with those described by Wu et al. in that all exhibited good adhesion [18]. Through these experiments, the application of DESP-CS as a biomedical glue was worth researching in the future.

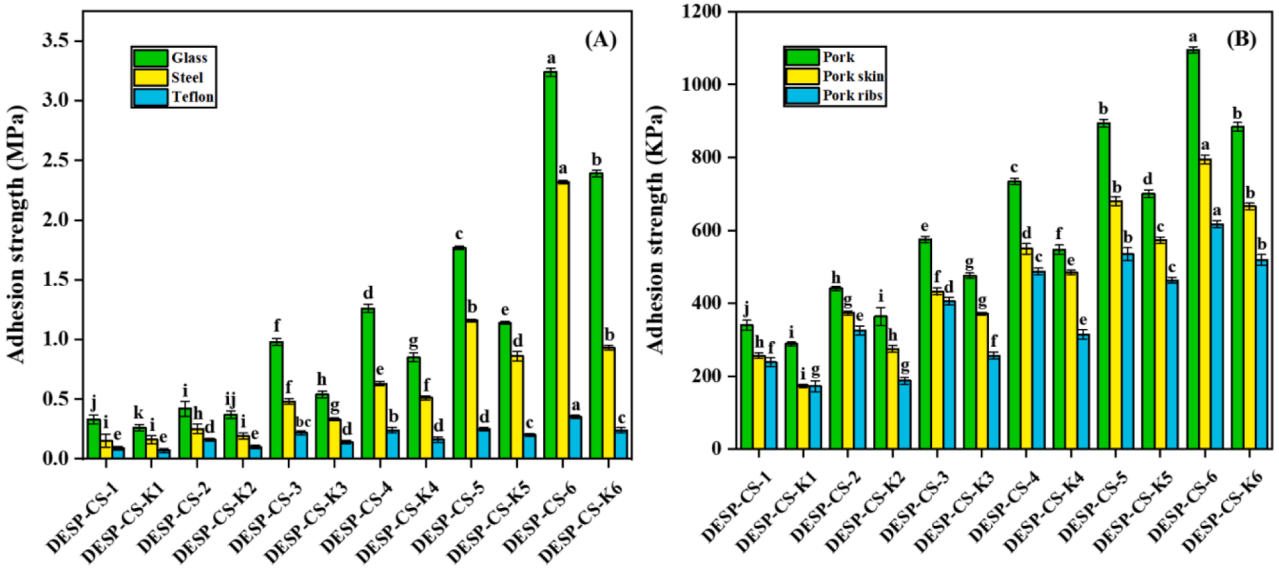

Fig. 9. Adhesion strength of DESP-CS on different substrates: (A) non-animal tissue, (B) animal tissue.

4. Conclusion

This study revealed the feasibility of DESP as an extractant and demonstrated that the combination of UAE with DESP is a novel, green and efficient method for the extraction of plant polyphenols. And the degradable biofilm prepared by blending CS with DESP extract as a dissolving agent and plasticizer can not only improve the mechanical properties of CS film, enhance the anti-plasticity ability, but also have the adhesion effect of supramolecular polymer, which can quickly and firmly adhere to animal tissues together. Therefore, this work shows that it is possible to reduce the tedious procedures for separating biologically active substances from DESP. According to the requirement of different applications, DESP-CS were designed and prepared with the addition of DESP and bioactive substances, which provided a new strategy for the green development of biofilm materials.

CRediT authorship contribution statement

Feng Shi: Writing – original draft, Conceptualization, Investigation. **Xiaoping Hai:** Data curation, Validation. **Yun Zhu:** Visualization. **Lei Ma:** Validation. **Lina Wang:** Visualization, Formal analysis. **Jinfang Yin:** Formal analysis. **Xiaofen Li:** Resources. **Zhi Yang:** Resources, Formal analysis. **Mingwei Yuan:** Supervision. **Huabin Xiong:** Writing – review & editing, Data curation. **Yuntao Gao:** Project administration, Resources.

Declaration of Competing Interest

The authors declare that they have no known competing financial interests or personal relationships that could have appeared to influence the work reported in this paper.

Acknowledgment

This work was supported by the National Natural Science Foundation of China [grant numbers: No.52163013] and Yunnan Province “Thousand Talents Program” project training project [grant numbers: YNQR-CYRC-2018-012].

Appendix A. Supplementary data

Supplementary data to this article can be found online at https://doi.org/10.1016/j.ultsonch.2022.106283.

References

[1] R.M. Wang, L.L. Yao, X. Lin, X.P. Hu, L. Wang, Exploring the potential mechanism of Rhodomyrtus tomentosa (Ait.) Hassk fruit phenolic rich extract on ameliorating nonalcoholic fatty liver disease by integration of transcriptomics and metabolomics profiling, Food Res. Int. 151 (2022) 13, https://doi.org/10.1016/j.foodres.2021.110824.

[2] C.Q. Zhu, C. Feng, X. Li, C.J. Xu, C.D. Sun, K.S. Chen, Analysis of expressed sequence tags from Chinese bayberry fruit (Myrica rubra Sieb. and Zucc.) at different ripening stages and their association with fruit quality development, Int. J. Mol. Sci. 14 (2013) 3110–3123, https://doi.org/10.3390/ijms14023110.

[3] Y. Zhu, J. Lv, Y. Gu, Y. He, J. Chen, X. Ye, Z. Zhou, Mixed fermentation of Chinese bayberry pomace using yeast, lactic acid bacteria and acetic acid bacteria: Effects on color, phenolics and antioxidant ingredients, Lwt 163 (2022), https://doi.org/10.1016/j.lwt.2022.113503.

[4] S.B. Ge, L.S. Wang, J.J. Ma, S.C. Jiang, W.X. Peng, Biological analysis on extractives of bayberry fresh flesh by GC-MS, Saudi, J. Biol. Sci. 25 (2018) 816–818, https://doi.org/10.1016/j.sjbs.2017.09.001.

[5] V. Spinola, E.J. Llorent-Martinez, S. Gouveia, P.C. Castilho, Myrica faya: A new source of antioxidant phytochemicals, J. Agric. Food Chem. 62 (2014) 9722–9735, https://doi.org/10.1021/jf503540s.

[6] H.H. Guo, R.M. Zhong, Y.J. Liu, X.W. Jiang, X.L. Tang, Z. Li, M. Xia, W.H. Ling, Effects of bayberry juice on inflammatory and apoptotic markers in young adults with features of non-alcoholic fatty liver disease, Nutrition 30 (2014) 198–203, https://doi.org/10.1016/j.nut.2013.07.023.

[7] V. Spinola, E.J. Llorent-Martinez, P.C. Castilho, Polyphenols of Myrica faya inhibit key enzymes linked to type II diabetes and obesity and formation of advanced glycation end-products (in vitro): Potential role in the prevention of diabetic complications, Food Res. Int. 116 (2019) 1229–1238, https://doi.org/10.1016/j.foodres.2018.10.010.

[8] H.H. Yang, Y.Q. Ge, Y.J. Sun, D.H. Liu, X.Q. Ye, D. Wu, Identification and characterisation of low-molecular-weight phenolic compounds in bayberry (Myrica rubra Sieb. et Zucc.) leaves by HPLC-DAD and HPLC-UV-ESIMS, Food Chem. 128 (2011) 1128–1135, https://doi.org/10.1016/j.foodchem.2011.03.118.

[9] C.D. Sun, H.Z. Huang, C.J. Xu, X. Li, K.S. Chen, Biological activities of extracts from Chinese bayberry (Myrica rubra Sieb et Zucc.): A Review, Plant Food Hum. Nutr. 68 (2013) 97–106, https://doi.org/10.1007/s11130-013-0349-x.

[10] J.S. Bao, Y.Z. Cai, M. Sun, G.Y. Wang, H. Corke, Anthocyanins, flavonols, and free radical scavenging activity of Chinese bayberry (Myrica rubra) extracts and their color properties and stability, J. Agric. Food Chem. 53 (2005) 2327–2332, https://doi.org/10.1021/jf048312z.

[11] Z.F. Yang, S.F. Cao, Y.H. Zheng, Chinese bayberry fruit extract alleviates oxidative stress and prevents 1,2-dimethylhydrazine-induced aberrant crypt foci development in rat colon carcinogenesis, Food Chem. 125 (2011) 701–705, https://doi.org/10.1016/j.foodchem.2010.09.070.

[12] Y.L. Zhang, L.C. Kong, C.P. Yin, D.H. Jiang, J.Q. Jiang, J. He, W.X. Xiao, Extraction optimization by response surface methodology, purification and principal antioxidant metabolites of red pigments extracted from bayberry (Myrica rubra) pomace, LWT-Food Sci. Technol. 51 (2013) 343–347, https://doi.org/10.1016/j.lwt.2012.09.029.

[13] X.N. Zhang, H.Z. Huang, X.Y. Zhao, Q. Lv, C.D. Sun, X. Li, K.S. Chen, Effects of flavonoids-rich Chinese bayberry (Myrica rubra Sieb. et Zucc.) pulp extracts on

glucose consumption in human HepG2 cells, J. Funct. Food. 14 (2015) 144–153, https://doi.org/10.1016/j.jff.2015.01.030.
[14] R. Ahmadi, B. Hemmateenejad, A. Safavi, Z. Shojaeifard, A. Shahsavar, A. Mohajeri, M.H. Dokoohaki, A.R. Zolghadr, Deep eutectic-water binary solvent associations investigated by vibrational spectroscopy and chemometrics, Phys. Chem. Chem. Phys. 20 (2018) 18463–18473, https://doi.org/10.1039/c8cp00409a.
[15] A. Paiva, R. Craveiro, I. Aroso, M. Martins, R.L. Reis, A.R.C. Duarte, Natural deep eutectic solvents - solvents for the 21st century, ACS Sustain. Chem. Eng. 2 (2014) 1063–1071, https://doi.org/10.1021/sc500096j.
[16] S.C. Cunha, J.O. Fernandes, Extraction techniques with deep eutectic solvents, Trac-Trends, Anal. Chem. 105 (2018) 225–239, https://doi.org/10.1016/j.trac.2018.05.001.
[17] R. Ahmadi, B. Hemmateenejad, A. Safavi, Z. Shojaeifard, M. Mohabbati, O. Firuzi, Assessment of cytotoxicity of choline chloride-based natural deep eutectic solvents against human HEK-293 cells: A QSAR analysis, Chemosphere 209 (2018) 831–838, https://doi.org/10.1016/j.chemosphere.2018.06.103.
[18] S.G. Wu, C.Y. Cai, F.F. Li, Z.J. Tan, S.Y. Dong, Deep eutectic supramolecular polymers: Bulk supramolecular mMaterials, Angew. Chem.-Int. Edit. 59 (2020) 11871–11875, https://doi.org/10.1002/anie.202004104.
[19] K.M. Jeong, J. Ko, J. Zhao, Y. Jin, D.E. Yoo, S.Y. Han, J. Lee, Multi-functioning deep eutectic solvents as extraction and storage media for bioactive natural products that are readily applicable to cosmetic products, J. Clean. Prod. 151 (2017) 87–95, https://doi.org/10.1016/j.jclepro.2017.03.038.
[20] B.K. Tiwari, Ultrasound: A clean, green extraction technology, Trac-Trends Anal. Chem. 71 (2015) 100–109, https://doi.org/10.1016/j.trac.2015.04.013.
[21] S. Koutsoukos, T. Tsiaka, A. Tzani, P. Zoumpoulakis, A. Detsi, Choline chloride and tartaric acid, a natural deep eutectic solvent for the efficient extraction of phenolic and carotenoid compounds, J. Clean. Prod. 241 (2019) 11, https://doi.org/10.1016/j.jclepro.2019.118384.
[22] C.M.R. Almeida, J. Magalhaes, H.K.S. Souza, M.P. Goncalves, The role of choline chloride-based deep eutectic solvent and curcumin on chitosan films properties, Food Hydrocoll. 81 (2018) 456–466, https://doi.org/10.1016/j.foodhyd.2018.03.025.
[23] J.-Š.-K.-J. Kristl, E. Štruc, M. Schara, H. Rupprecht, Hydrocolloids and gels of chitosan as drug carriers, Int. J. Pharmaceut. 99 (1993) 13–19, https://doi.org/10.1016/0378-5173(93)90317-9.
[24] M.G.A. Vieira, M.A. da Silva, L.O. dos Santos, M.M. Beppu, Natural-based plasticizers and biopolymer films: A review, Eur. Polym. J. 47 (2011) 254–263, https://doi.org/10.1016/j.eurpolymj.2010.12.011.
[25] M.P. Sokolova, M.A. Smirnov, A.A. Samarov, N.V. Bobrova, V.K. Vorobiov, E. N. Popova, E. Filippova, P. Geydt, E. Lahderanta, A.M. Toikka, Plasticizing of chitosan films with deep eutectic mixture of malonic acid and choline chloride, Carbohydr. Polym. 197 (2018) 548–557, https://doi.org/10.1016/j.carbpol.2018.06.037.
[26] V.C. Roy, A.T. Getachew, Y.-J. Cho, J.-S. Park, B.-S. Chun, Recovery and bio-potentialities of astaxanthin-rich oil from shrimp (Penaeus monodon) waste and mackerel (Scomberomous niphonius) skin using concurrent supercritical CO_2 extraction, J. Supercrit. Fluid. 159 (2020), https://doi.org/10.1016/j.supflu.2020.104773.
[27] V.C. Roy, T.C. Ho, H.J. Lee, J.S. Park, S.Y. Nam, H. Lee, A.T. Getachew, B.S. Chun, Extraction of astaxanthin using ultrasound-assisted natural deep eutectic solvents from shrimp wastes and its application in bioactive films, J. Clean. Prod. 284 (2021) 10, https://doi.org/10.1016/j.jclepro.2020.125417.
[28] L.F. Wu, L. Li, S.J. Chen, L. Wang, X. Lin, Deep eutectic solvent-based ultrasonic-assisted extraction of phenolic compounds from Moringa oleifera L. leaves: Optimization, comparison and antioxidant activity, Sep. Purif. Technol. 247 (2020) 11, https://doi.org/10.1016/j.seppur.2020.117014.
[29] W. Vongsangnak, J. Gua, S. Chauvatcharin, J.J. Zhong, Towards efficient extraction of notoginseng saponins from cultured cells of Panax notoginseng, Biochem. Eng. J. 18 (2004) 115–120, https://doi.org/10.1016/s1369-703x(03)00197-9.
[30] J. Huang, X.Y. Guo, T.Y. Xu, L.Y. Fan, X.P. Zhou, S.H. Wu, Ionic deep eutectic solvents for the extraction and separation of natural products, J. Chromatogr. A 1598 (2019) 1–19, https://doi.org/10.1016/j.chroma.2019.03.046.
[31] X. Rico, E.M. Nuutinen, B. Gullon, V. Pihlajaniemi, R. Yanez, Application of an eco-friendly sodium acetate/urea deep eutectic solvent in the valorization of melon by-products, Food Bioprod. Process. 130 (2021) 216–228, https://doi.org/10.1016/j.fbp.2021.10.006.
[32] F. Chemat, N. Rombaut, A.G. Sicaire, A. Meullemiestre, A.S. Fabiano-Tixier, M. Abert-Vian, Ultrasound assisted extraction of food and natural products. Mechanisms, techniques, combinations, protocols and applications. A review, Ultrason. Sonochem. 34 (2017) 540–560, https://doi.org/10.1016/j.ultsonch.2016.06.035.
[33] L. Wu, L. Li, S. Chen, L. Wang, X. Lin, Deep eutectic solvent-based ultrasonic-assisted extraction of phenolic compounds from Moringa oleifera L. leaves: Optimization, comparison and antioxidant activity, Sep. Purif. Technol. 247 (2020), https://doi.org/10.1016/j.seppur.2020.117014.
[34] M.-C. Wei, Y.-C. Yang, Extraction characteristics and kinetic studies of oleanolic and ursolic acids from *Hedyotis diffusa* under ultrasound-assisted extraction conditions, Sep. Purif. Technol. 130 (2014) 182–192, https://doi.org/10.1016/j.seppur.2014.04.029.
[35] L.C. Favre, G. Rolandelli, N. Mshicileli, L.N. Vhangani, C.D. Ferreira, J. van Wyk, M.D. Buera, Antioxidant and anti-glycation potential of green pepper (Piper nigrum): Optimization of beta-cyclodextrin-based extraction by response surface methodology, Food Chem. 316 (2020) 11, https://doi.org/10.1016/j.foodchem.2020.126280.
[36] M.S. Chen, Y. Zhao, S.J. Yu, Optimisation of ultrasonic-assisted extraction of phenolic compounds, antioxidants, and anthocyanins from sugar beet molasses, Food Chem. 172 (2015) 543–550, https://doi.org/10.1016/j.foodchem.2014.09.110.
[37] S. Nipornram, W. Tochampa, P. Rattanatraiwong, R. Singanusong, Optimization of low power ultrasound-assisted extraction of phenolic compounds from mandarin (Citrus reticulata Blanco cv. Sainampueng) peel, Food Chem. 241 (2018) 338–345, https://doi.org/10.1016/j.foodchem.2017.08.114.
[38] L.C. Favre, C. dos Santos, M.P. Lopez-Fernandez, M.F. Mazzobre, M.D. Buera, Optimization of beta-cyclodextrin-based extraction of antioxidant and anti-browning activities from thyme leaves by response surface methodology, Food Chem. 265 (2018) 86–95, https://doi.org/10.1016/j.foodchem.2018.05.078.
[39] M.A. Bezerra, R.E. Santelli, E.P. Oliveira, L.S. Villar, L.A. Escaleira, Response surface methodology (RSM) as a tool for optimization in analytical chemistry, Talanta 76 (2008) 965–977, https://doi.org/10.1016/j.talanta.2008.05.019.
[40] T.E. Sintra, A. Luis, S.N. Rocha, A. Ferreira, F. Goncalves, L. Santos, B.M. Neves, M. G. Freire, S.P.M. Ventura, J.A.P. Coutinho, Enhancing the antioxidant characteristics of phenolic acids by their conversion into cholinium salts, ACS Sustain. Chem. Eng. 3 (2015) 2558–2565, https://doi.org/10.1021/acssuschemeng.5b00751.
[41] P. Zhao, J. Wang, X. Yan, Z. Cai, L. Fu, Q. Gu, L. Liu, H. Jin, Y. Fu, Functional chitosan/zein films with *Rosa roxburghii* Tratt leaves extracts prepared by natural deep eutectic solvents, Food Packag. Shelf Life 34 (2022), https://doi.org/10.1016/j.fpsl.2022.101001.
[42] A.C. Galvis-Sanchez, M.C.R. Castro, K. Biernacki, M.P. Goncalves, H.K.S. Souza, Natural deep eutectic solvents as green plasticizers for chitosan thermoplastic production with controlled/desired mechanical and barrier properties, Food Hydrocoll. 82 (2018) 478–489, https://doi.org/10.1016/j.foodhyd.2018.04.026.
[43] M. Kundu, S. Saha, M.N. Roy, Evidences for complexations of β-cyclodextrin with some amino acids by 1 H NMR, surface tension, volumetric investigations and XRD, J. Mol. Liq. 240 (2017) 570–577, https://doi.org/10.1016/j.molliq.2017.05.123.
[44] X. Han, Z. Zheng, C. Yu, Y. Deng, Q. Ye, F. Niu, Q. Chen, W. Pan, Y. Wang, Preparation, characterization and antibacterial activity of new ionized chitosan, Carbohydr Polym. 290 (2022), 119490, https://doi.org/10.1016/j.carbpol.2022.119490.
[45] A.S.B.D. Sousa, R.P. Lima, M.C.A.D. Silva, D.D.N. Moreira, M.M.E. Pintado, S.D. M. Silva, Natural deep eutectic solvent of choline chloride with oxalic or ascorbic acids as efficient starch-based film plasticizers, Polymer 259 (2022), https://doi.org/10.1016/j.polymer.2022.125314.
[46] X. Zhang, Y. Zhao, Y.Y. Li, L.L. Zhu, Z.X. Fang, Q.L. Shi, Physicochemical, mechanical and structural properties of composite edible films based on whey protein isolate/psyllium seed gum, Int. J. Biol. Macromol. 153 (2020) 892–901, https://doi.org/10.1016/j.ijbiomac.2020.03.018.
[47] D.G. Ramirez-Wong, M. Ramirez-Cardona, R.J. Sanchez-Leija, A. Rugerio, R. A. Mauricio-Sanchez, M.A. Hernandez-Landaverde, A. Carranza, J.A. Pojman, A. M. Garay-Tapia, E. Prokhorov, J.D. Mota-Morales, G. Luna-Barcenas, Sustainable-solvent-induced polymorphism in chitin films, Green Chem. 18 (2016) 4303–4311, https://doi.org/10.1039/c6gc00628k.
[48] F. Xue, M. Zhao, X. Liu, R. Chu, Z. Qiao, C. Li, B. Adhikari, Physicochemical properties of chitosan/zein/essential oil emulsion-based active films functionalized by polyphenols, Future Foods 3 (2021), https://doi.org/10.1016/j.fufo.2021.100033.